Design and optimization of acoustic liners with a shear grazing flow: OPAL software applications

Rémi Roncen, Pierre Vuillemin, Patricia Klotz, Frank Simon, Fabien Méry, Delphine Sebbane, Estelle Piot

Design and optimization of acoustic liners with a shear grazing flow : OPAL software applications

Rémi Roncen[1†], Pierre Vuillemin[2‡], Patricia Klotz[3‡], Frank Simon[4†], Fabien Méry[5†], Delphine Sebbane[6†], Estelle Piot[7†]
[†]ONERA/DMPE, Université de Toulouse, F-31055, Toulouse, France
[‡]ONERA/DTIS, Université de Toulouse F-31055, Toulouse, France

ABSTRACT

A software platform named OPAL was developed to perform multi-objective optimization of meta-surface acoustic liners. This paper focuses on different numerical aspects of liner design. A numerical analysis is conducted, mimicking an acoustic project. OPAL's goal is to allow the user to assemble a large panel of parallel/serial assemblies of unit acoustic elements (foams, perforated plates, cavities, etc.). The material properties are then optimized relatively to given weighted objectives (noise reduction, total size of the sample). In the present applications, noise reduction is predicted on some reference configurations, which are computed with a 2D high-order Discontinuous Galerkin resolution of the linearised Euler equations, coupled with a reduced order model. Experimental results are also given for the transmission loss realised by a meta-surface created during the development of OPAL.

1. INTRODUCTION

Operational constraints in the aeronautical field impose an ever more stringent reduction of the noise levels emitted by airplanes. This noise reduction is generally achieved in the engine nacelle by the integration of acoustic materials called liners, which work on the principle of an acoustic resonator and attenuate part of the acoustic waves. Locally reacting liners are well characterized, acoustically speaking, by their impedance Z [1], a frequency dependent operator linking the acoustic pressure p and normal velocity v_n as

$$Z = \frac{p}{v_n}. \tag{1}$$

[1]remi.roncen@onera.fr
[2]pierre.vuillemin@onera.fr
[3]patricia.klotz@onera.fr
[4]frank.simon@onera.fr
[5]fabien.mery@onera.fr
[6]delphine.sebbane@onera.fr
[7]estelle.piot@onera.fr

The development of acoustic liners with an innovative architecture is part of the progress sought to meet the acoustic challenges of tomorrow. For this purpose, a python module named OPAL (OPtimization of Acoustic Liners) is currently being developed at ONERA, in order to assemble the different elements allowing the design of novel acoustic liners. Some of these elements are:

- Freedom to assemble a liner with various acoustical unit elements.
- Evaluate the acoustic behaviour of a meta-surface composed of a parallel assembly of multi-layer materials.
- Evaluate the optimal impedance in a given system in the presence of a flow, at low cost.
- Identify the properties of a liner that best realize an optimal impedance, under constraints and/or multiple objectives.

This paper focuses on presenting the above items in action with OPAL on a synthetic numerical case. The software architecture is first summarized in Sec. 2, but more details can be found in the companion proceeding entitled "Design and optimization of acoustic liners with a shear grazing flow: OPAL software platform description", by F. Simon et. al. Then, in Sec. 3, a numerical example is shown where various acoustic liner are optimized for a given application, i.e., shear grazing flow with average Mach of 0.2, high sound pressure level (SPL) of 140dB. Experiments are conducted in ONERA's B2A aeroacoutsic bench, with a complex meta-surface assembly. A brief presentation of this experiment is given in Sec. 4, followed by a discussion in Sec. 5. Conclusions are drawn in Sec. 6.

2. THE OPAL SOFTWARE

Written in python 3, OPAL is a library containing three modules:

- The *sandbox* module is dedicated to the creation and assembly of acoustic unit elements, such as a perforated plate, a foam, a cavity.
- The *mamout* module is dedicated to the definition and solving of the linearised Euler equations (LEE) in 1D, assuming a liner with infinite dimensions in all but one direction.
- The *pyDG* module is dedicated to the definition and solving of the LEE in 2D, using a high order Discontinuous-Galerkin (DG) scheme.

Once the user has assembled a given liner, specifying what materials to use and what environment the liner is located in (ambient fluid properties, presence of a flow, SPL, frequency range), its impedance (or other acoustic properties) can be estimated. The user can then optimize the selected liner configuration (or choose within a dedicated library of liner candidates) for a given system, using either 1D or 2D simulations with free and open-source optimization softwares that have been interfaced with OPAL [2, 3].

The *sandbox* and *pyDG* modules listed previously are detailed in the following, as they are extensively used in the applications presented in this paper.

2.1. The *sandbox* module

Using the transfer matrix method of Ref. [4, Chap. 11], one can evaluate the surface impedance of any combination of materials forming a multi-layer (serial assembly). In the *sandbox* module, only equivalent fluid materials are considered. This covers in practice a vast range of different materials, listed in the following for completeness.

– Rigid porous materials, such as foams, can be accurately represented acoustically by an equivalent fluid [4]. Different semi-phenomenological models exist to predict how waves propagate in such materials, as a function of the pore network intrinsic properties (porosity, tortuosity, etc.). This includes the JCAPL model (Johnson-Champoux-Allard-Pride-Large) [5–8] and its earlier versions, the JCA and JCAL models.

– Rigid perforated plates can also be represented as porous materials, and thus as equivalent fluids. However, due to end effects occurring at the perforations, some corrections need to be taken into account for the equivalent tortuosity of the material, as done in Ref. [9].

– Cavities, such as honeycomb layers, can also be seen as porous materials (albeit, of very high porosity and pore radius). Alternatively, they can be considered as fluid layers.

– LEONAR materials, which are made from a tube that extends inside a cavity [10,11], are simply the combination of two unit materials (tube and cavity), and can be represented by the transfer matrix of two equivalent fluids stacked together as a first approximation. In practice, this is not exact due to the presence of tubes in the cavity "hiding" some of the cavity volume [12].

Given different multi-layers, the user can then assemble a meta-surface liner (parallel assembly of impedances), where the total impedance becomes

$$Z_{\text{tot}} = \left(\sum_i \frac{\Psi_i}{Z_i} \right)^{-1}, \tag{2}$$

where Ψ_i is the surface ratio of each multi-layer within the liner ($\sum_i \Psi_i = 1$) and where Z_i is the impedance of the i-th multi-layer. A schematics is shown in Fig. 1

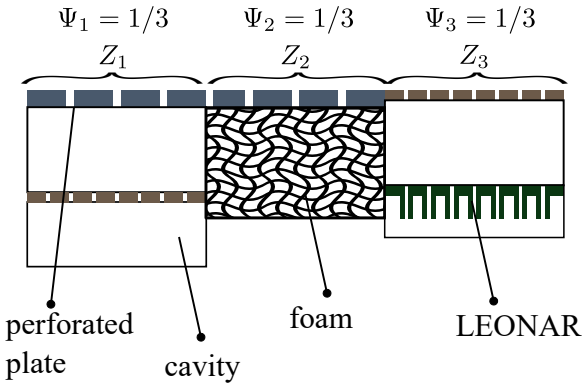

Figure 1: Schematics of a meta-surface made of three different multi-layers. Ψ_i is the surface ratio of each multi-layer cell in the liner. The meta-surface pattern is assumed to repeat indefinitely, yielding the homogenized impedance of Eq. 2.

Note that Eq. 2 only holds when the wavelength is large compared with the size of the meta-surface pattern so that the locally-reacting assumption is verified. At high frequencies, the impedance cannot be homogenized, and impedance discontinuities must be taken into account.

Once the user has defined a liner (potentially made of any number of multi-layers), and once an environment is specified (frequency range, SPL, etc.), OPAL can yield the acoustic indicators of interest, such as the absorption coefficient or the impedance, using the transfer matrix approach and Eq. 2. Nonlinear effects, caused by a high SPL or the presence of the flow, are accounted for by prescribing which model to use for each element composing the liner, among a selection from the literature [13–15], or any user defined model.

The *sandbox* module also embeds functions to translate automatically the aforementioned physical description of the liner to a standard mathematical form of the optimisation problem shared by most existing solvers. In particular, the objective is to minimize (or maximize) some (user-defined) function $f(\boldsymbol{x})$ under some inequality constraints $c(\boldsymbol{x}) \leq 0$ (bounds on parameters and thickness of the liner) where $\boldsymbol{x}$ is a vector gathering all the physical parameters of the liner. Later in Sec. 3, some examples are given concerning the choice of f which can translate various design choices.

2.2. The *pyDG* module

Most of the heavy lifting in OPAL comes from the *pyDG* module, where the user can define a 2D geometry on which to solve the LEE in the harmonic regime, or any set of user-defined hyperbolic partial derivative equations (PDE). A high-order DG scheme is proposed, with high-order quadrature rules to avoid aliasing errors when a non-constant background field (shear flow, space-dependent impedance [16]) is chosen.

The LEE, written in non-conservative form with an $e^{j\omega t}$ time dependence and assuming homentropic flow, are given by

$$\mathrm{j}\omega\boldsymbol{\varphi} + \boldsymbol{A}_x\partial_x\boldsymbol{\varphi} + \boldsymbol{A}_y\partial_y\boldsymbol{\varphi} + \boldsymbol{B}\boldsymbol{\varphi} = \boldsymbol{S}, \tag{3}$$

where

$$\boldsymbol{A}_x = \begin{pmatrix} U & 0 & c_0 \\ 0 & U & 0 \\ c_0 & 0 & U \end{pmatrix},\ \boldsymbol{A}_y = \begin{pmatrix} V & 0 & 0 \\ 0 & V & c_0 \\ 0 & c_0 & V \end{pmatrix},\ \boldsymbol{B} = \begin{pmatrix} \partial_x U & \partial_y U & 0 \\ \partial_x V & -\partial_x U & 0 \\ 0 & 0 & 0 \end{pmatrix},$$

with $\boldsymbol{S}$ a source vector. U and V are the x and y mean flow velocity components, respectively, and c_0 is the speed of sound of the ambient fluid (air). Components of the state vector $\boldsymbol{\varphi} = \left(u, v, \frac{p}{\rho_0 c_0}\right)$ represent the acoustic perturbations around the mean flow, with u, v the particle axial and transverse velocity, p the particle pressure and ρ_0 the mean flow density. Due to the homentropy condition, the energy equation is replaced by the state equation $p = c_0^2\rho$, with ρ the density perturbation around the mean.

The details of the DG method for the solving of the LEE with an impedance boundary condition (BC) are given in Refs. [17, 18], and are mostly derived from the introductory book on the subject by Hesthaven [19]. Overall, the *pyDG* module reads the mesh discretization, assembles the linear system and solves it with the scipy library [2].

When transverse calculations are undertaken (i.e., in the cross section), an eigenproblem is solved to find the duct modes wave-numbers. More information can be found in Ref. [20], where an earlier version of OPAL had been used at the time.

2.2.1. Snapshot-POD for faster calculations

Without any acceleration, solving a 2D LEE problem may take a few seconds at each frequency of interest, depending on the size of the mesh and the DG cell order that was chosen. While this may seem fast enough when simply trying to evaluate the solution associated with a given impedance BC, it can become a problem in certain applications. For instance, optimization algorithms require many evaluation of the objective function, as well as impedance eduction problems (deterministic or statistical [18]).

This shortcoming is addressed by the projection of the discretized LEE onto a reduced order basis [21], based on proper orthogonal decomposition (POD). The basis is created by the evaluation of the true solution at different impedance values (or any other parameter such as the source amplitude, or even the frequency). These solutions, called snapshots, are assembled to form an orthogonal matrix of size $N_{\mathrm{sol}} \times N_{\mathrm{ROM}}$, where N_{sol} is the full size of the solution, and N_{ROM} is typically a low number associated with the reduced order model (ROM) ($N_{\mathrm{ROM}} \leq$ the number of snapshots that were

calculated). In our examples, $N_{\text{ROM}} = 10 - 20$ is usually sufficient to create an accurate basis. This accuracy is checked a posteriori by the comparison between the ROM and the true solution (i.e., without model reduction), at various impedances that were not used during the creation of the basis. The method is coined snapshot-POD.

Once the projection onto this new basis is done, the problem becomes that of solving a linear system of size $N_{\text{ROM}} \times N_{\text{ROM}}$, which is almost instantaneous when compared to the initial cost. Details on the method and its application on statistical inference for impedance eduction can be found in Ref. [18].

3. LINER OPTIMIZATION PROCEDURE

A numerical test case is treated here that displays the general approach followed in OPAL for liner design. The acoustic system considered for this example is ONERA's B2A aeroacoustic bench, a duct of 5cm by 5cm square cross section, where a shear grazing flow up to Mach 0.4 and a SPL up to 150dB can be used (see Fig. 2). A 15cm long liner can be placed within the duct, and the present goal is to maximize the attenuation performed by the liner. The incident acoustic waves propagates in the same direction as the flow. An average Mach number of $M_a = 0.2$ is considered for the test case (see

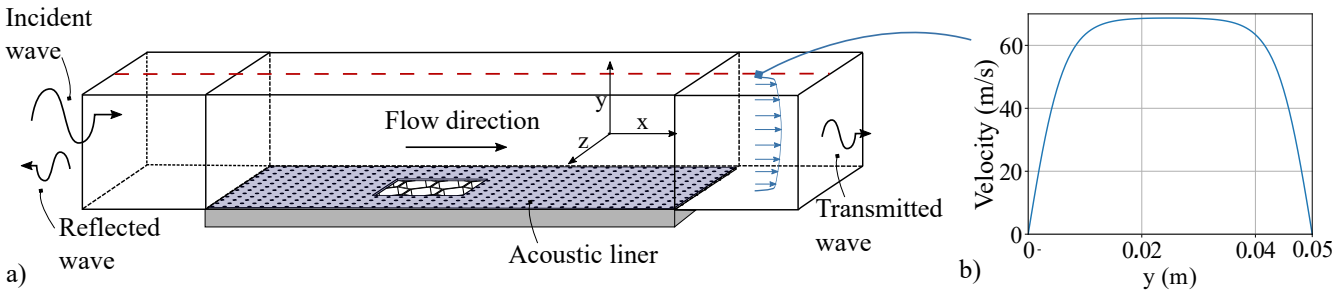

Figure 2: a) Schematics of ONERA's B2A aeroacoustic bench (not to scale). The red dashed line indicates the position where pressure measurements are taken. b) Shear grazing flow profile.

Fig. 2.b for the flow profile). The frequency range of interest is [200Hz-3000Hz] with a step of 10Hz, with a more important weight at 500Hz representing the designer's wish to attenuate sound at this frequency with a higher priority. In practice, one can specify a noise spectrum as input to weigh the frequencies during the optimization process. More details are given in the following. In the present work, only the 2D test-case is investigated, i.e., the (x, y) plane at the center of the test section. Any 3D effect is neglected.

The first step is for OPAL to assemble the 2D DG problem, given a mesh geometry and a cell order. This is taken care of by the *pyDG* module. The mesh around the impedance BC is shown in Fig. 3. Once the user has specified the shear grazing flow profile, the linear system resulting from the DG

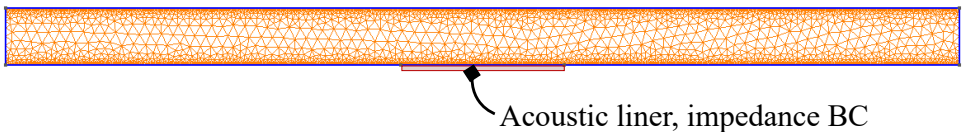

Figure 3: Mesh created by GMSH [22] and used by the *pyDG* module for the discretization of the LEE.

discretization of the LEE is created. A numerical trick is used here, where the matrices involved are split in order to extract the contribution of parameters that may vary in the simulations (for instance,

the impedance). This allows one to not have to re-build entirely the linear system every time the impedance is changed.

At each frequency of interest, a snapshot-POD surrogate basis is created iteratively (see Sec. 1, or Ref. [18] for more details). N_Z impedance values are used, at which the solution (called snapshot) is evaluated and stored. When the N_Z calculations have been performed, the matrix containing all the snapshot solutions is orthogonalized and saved. The choice of N_Z depends on the problem complexity, and is fixed here at $N_Z = 19$. Instead of selecting the impedance value, which is unbounded, we rather select the reflection coefficient value β_s, which is defined as

$$\beta_s = \frac{Z - 1}{Z + 1}, \tag{4}$$

where Z is taken here as the normalized impedance (same convention is followed hereafter). The values of reflection coefficients are sampled in the complex unit disk, as shown in Fig. 4.

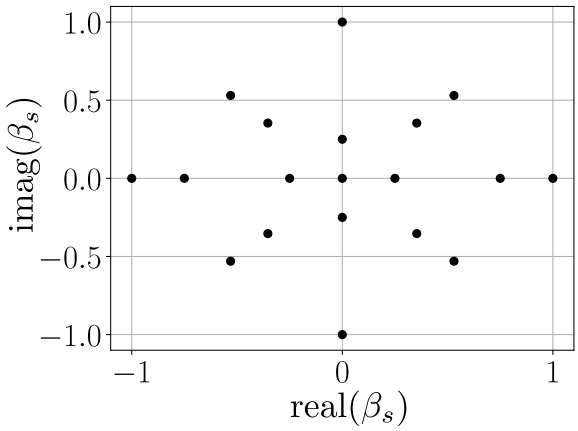

Figure 4: Sample points used to calculate the snapshots.

In the present case, the speed-up factor obtained with the ROM is of the order of $10^3 - 10^4$. The precision is evaluated by comparing the true solution to the ROM solution at different impedances that where not part of the basis creation, yielding a relative error on all fields (pressure and velocity) not exceeding a fraction of a percent.

Using the ROM, the transmission loss (TL) can be evaluated cheaply, at any impedance. The TL is defined as

$$\mathrm{TL} = \mathrm{SPL}_{in} - \mathrm{SPL}_{out}, \tag{5}$$

where SPL_{in} is a user defined input and where SPL_{out} is evaluated near the mesh outlet. An optimal impedance, i.e., that yields the highest TL, can thus be evaluated at each frequency. A map of this TL is showed in Fig. 5 at 1500Hz, where 40×10^3 data points were calculated using the ROM, in about 2min. To evaluate the TL of a given liner at all frequencies, a nearest-neighbour algorithm is used to extract the TL value from the pre-calculated TL maps. Note that some spurious solutions can be obtained with the ROM, as seen in Fig. 5 near $\beta_s = -1$. If necessary, the user can add a new snapshot in this area to increase the precision where needed, iteratively improving the reduced basis.

Now that the TL maps are saved, there are different ways to perform the liner optimization, that can lead to various solutions. One such strategy would be to try to maximize the TL realized by the liner at each frequencies ω, i.e. $f_0(\boldsymbol{x}) = \max_\omega TL$. However, this tends to favour a liner design that is efficient at high frequencies, if nothing is done to enforce acoustic absorption of the liner at low frequencies. That is partly because at high frequencies, the wavelength is lower, and hence "sees" the liner for more spatial periods. Another strategy would be to only optimize the impedance value (or in this case, the reflection coefficient), to get as close to the optimal value β_{opt} as possible, i.e.

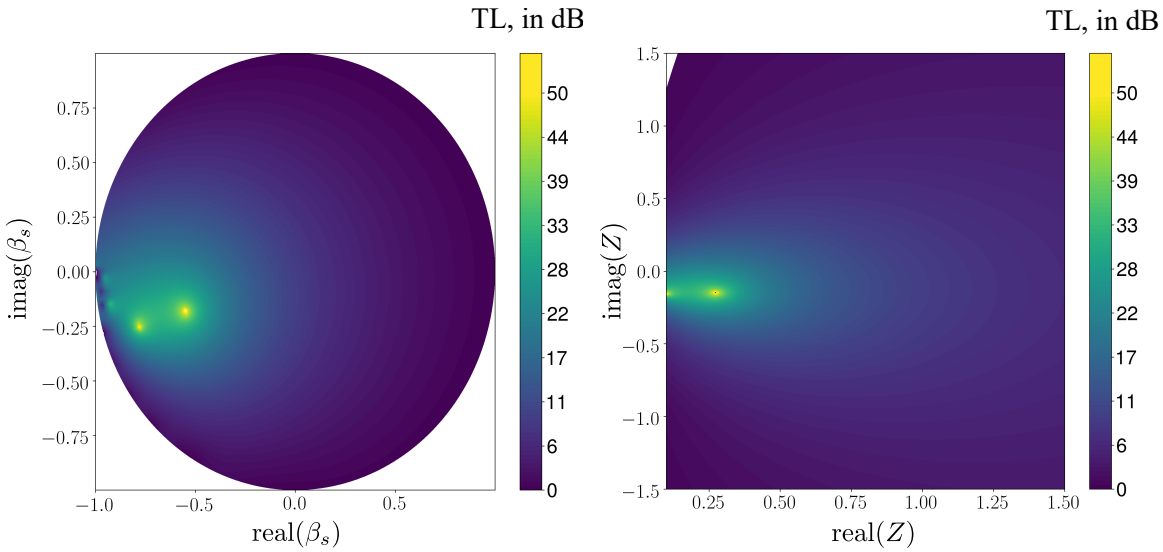

Figure 5: TL map at 1500Hz, in the reflection coefficient space (left) and the (reduced) impedance space (right).

$f_1(\boldsymbol{x}) = \min \sum_\omega |\beta(\boldsymbol{x}, \omega) - \beta_{\text{opt}}(\omega)|$. The main drawback of this approach is that no information on the TL is given, which can enforce suboptimal solutions. Indeed, the TL variation (i.e., its gradient) around the optimal impedance value gives an estimate of the robustness of the solution.

As both objectives f_0 and f_1 are meaningful, one could consider them both within a multi-objective optimization to be solved with dedicated methods such as those available in pyMOO [3]. Otherwise, one can also stick with mono-objective optimisation by using a scalarisation approach. More specifically, a compromise objective f is formed as a weighted sum of both f_0 and f_1, as follows.

The optimal reflection coefficient is selected as the main target. A first weighting is performed on frequencies, giving more weight when the optimal TL is steep, which indicates that an error on the reflection coefficient would be more damaging to the overall absorption of the liner. Finally, a second weighting is performed to translate the user interest in the particular frequency of 500Hz, using the TL calculated at this frequency. The user can then enforce a minimal threshold of attenuation at this given frequency. The setting of this particular weight α_{500} is crucial. If set too low, it will have no effect on the output. However, if set too high, the other frequencies won't be considered during the optimization. To palliate this and avoid a tedious parameter selection process, a very high value of α_{500} is taken, but a TL threshold is fixed. Remains the possibility that the algorithm could not reach a solution where the required attenuation threshold is achieved. The cost function that is minimized is the following:

$$f = \sum_i \epsilon_i \left|\beta_{s,\text{optim}}(\omega_i) - \beta_s(\omega_i)\right|^2 + \alpha_{500} \min\left(\text{TL}(500\text{Hz}), \text{TL}_{\text{threshold}}\right), \tag{6}$$

where ϵ_i is a measure of how peaked the TL surface is in the TL maps, $\beta_{s,\text{optim}}(\omega_i)$ is the optimal reflection coefficient, found on the TL maps, $\beta_s(\omega_i)$ is the candidate liner's reflection coefficient, and α_{500} is a user defined weight to bias the optimization towards solutions that yield some attenuation at 500Hz. Note that the purpose of the min function next to α_{500} is to stop the optimization from trying to increase the TL at the specified frequency above a given user defined threshold $\text{TL}_{\text{threshold}}$, which would be done at the detriment of the other frequencies. In practice, different threshold values are tried, and the best design can be chosen by the user at the end (visual inspection of the TL over the frequency range, calculation of other indicators, lowest thickness candidate, etc.). All these secondary objectives, that guide the liner selection, can be integrated using the multi-objective optimization package pyMOO [3].

3.1. Optimisation results

In total, 15 different liner candidates were considered, as part of OPAL's standard liner library. For brevity, only 3 different design candidates are selected for display here. On all designs, a wiremesh was added (assumed to be a thin porous media, following Ref. [9]. This is done in practice to limit the influence of the flow on the liner acoustic behaviour [23].

- Liner 1 : a parallel assembly of 6 different single degree of freedom liners (SDOF).
- Liner 2 : a triple degree of freedom liner (3 stacked SDOFs).
- Liner 3 : a parallel assembly of 6 different LEONAR samples.

Constraints: The total sample thickness constraint is imposed at 6cm (a linear system enforcing the constraints is assembled by the *sandbox* module, that can be given to an optimization algorithm or placed in the cost function by the user). Internal constraints (such as the one specifying that the tube length should not expect the cavity length in LEONAR samples) are also handled. While a user can decide to fix certain parameters or materials, all the parameters are considered during the present optimisation. Perforated plates are limited to a thickness of [0.5-2]mm, a porosity of [1-40]% and a radius of perforation of [0.5-2.5]mm. LEONAR tubes are limited in length by their cavity size (85%), a porosity of [1-15]% and an inner tube radius of [0.5-2.5mm]. Different parameter constraints would lead to different design solutions. The choice was broadly motivated here by manufacturability conditions.

Optimization: As sketched earlier, the resulting optimisation problem is a black-box non-linear optimisation problem with (linear) inequality constraints which can be plugged to various existing solvers. The problem may be differentiable depending on the considered objective function, but finite-differences should be considered with care. This is due to the complexity of the underlying chain of functions, relating the physical parameters $\boldsymbol{x}$ to the output of the numerical simulator f. From the authors' perspective, general purpose evolutionnary methods have proven to be more suitable for the problem. In addition to being derivative-free, these methods enable a wider (albeit arguably slower) exploration of the space of optimisation variables which fits the overall design purpose of the OPAL framework. In particular, the random nature of evolutionary methods prevents being prematurely stuck in local minima and offers a better chance at finding the global one. Under various assumptions, most of these methods enjoy asymptotic convergence properties. In the sequel, we consider a Genetic Algorithm that evolves within the search space by performing different bio-inspired operations on a set of candidate solutions (called population): mutation, crossover and selection.

Models The Guess model [14] was used for both the shear grazing flow effect on the wiremesh (usually a small effect) and the high SPL nonlinearity effect (total SPL is taken as 140dB), to update the impedance value. While the impedance is technically a function of space in the presence of nonlinear SPL effects [16], it was assumed constant here for simplicity (a space dependent impedance seems to limit the use of the snapshot-POD approach).

The optimization results are shown in Figs. 6, 7, 8, for different values of $\mathrm{TL}_{\mathrm{threshold}}$ ranging from 2dB to 10dB.

Analysis: All the proposed liners are able to reach a certain TL at 500Hz, as per the design goal. Liner 1 is only able to attain a solution reaching this constraint in one case, with some attenuation at higher frequencies. It is notable, however, that this solution should have been obtained more than once, with the higher values of $\mathrm{TL}_{\mathrm{threshold}}$. Since the optimization has some randomness to it, it should be repeated a couple times to ensure that the global minimum of Eq. 6 is obtained.

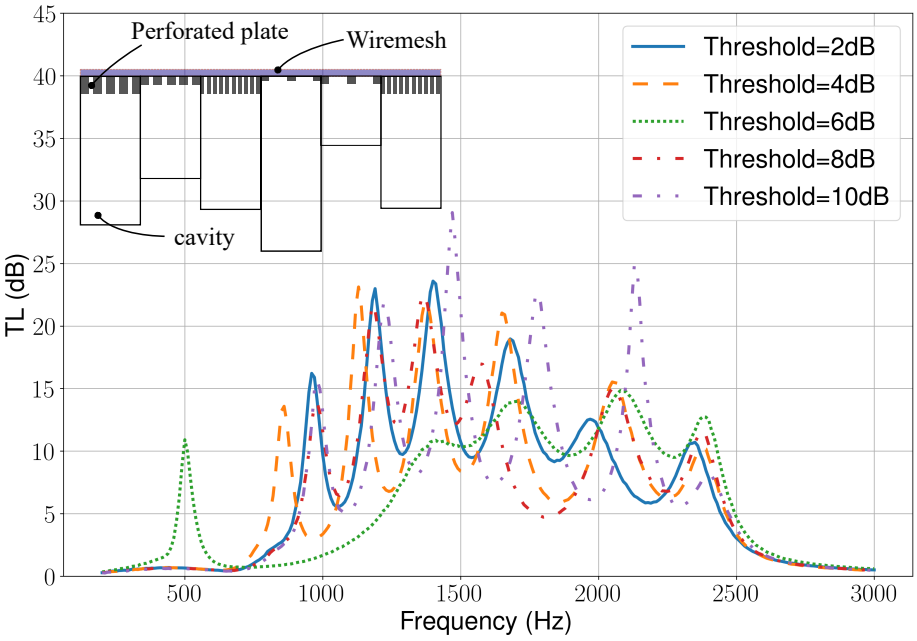

Figure 6: Optimized TL for liner 1 (length 15cm), a parallel assembly of 6 SDOF cells, with a wiremesh on top. Embedded schematics of the liner meta-surface.

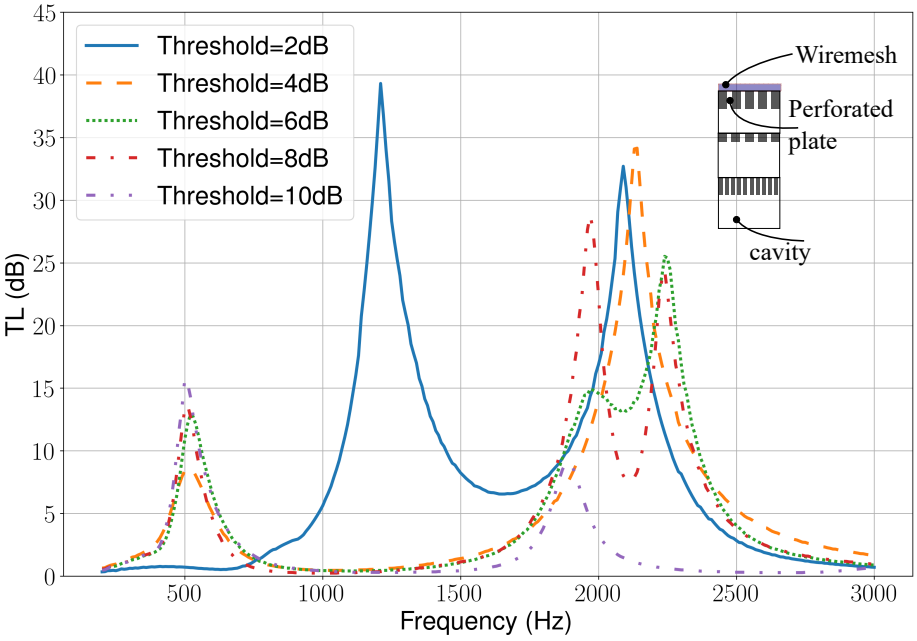

Figure 7: Optimized TL for liner 2 (length 15cm), a stacked assembly of 3 SDOFs cells, with a wiremesh on top. Embedded schematics of the liner multi-layer.

Liner 2, which is not a meta-surface but a multi-layer, has a less broadband behaviour than liner 1, as expected (no parallel homogenization). However, it is still able to provide some absorption at 500Hz, while remaining efficient at higher frequencies around 2kHz. In the case where the threshold TL is low, the optimization converges towards a solution that does not absorb at all at 500Hz but is rather effective at mid frequencies.

The parallel assembly of LEONAR samples (liner 3) is also able to reach the specified target TL at low frequency, while still yielding a correct TL at higher frequencies. Compared with solutions of

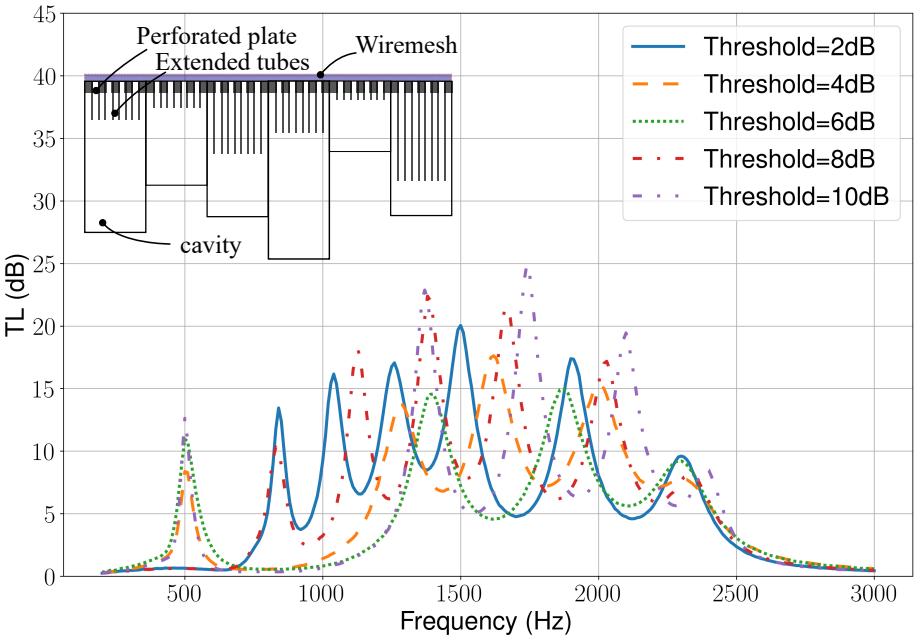

Figure 8: Optimized TL for liner 3 (length 15cm), a parallel assembly of 6 LEONAR cells, with a wiremesh on top. Embedded schematics of the liner meta-surface.

liner 1 and 2 that provide the required TL at 500Hz, liner 3 has a higher absorption in the frequency range $1 - 1.5$kHz.

Validity of the meta-surface impedance: While the *pyDG* module allows for calculations where multiple impedances are present (or even various zones with different equations solved in each), it is more practical to optimize the value of a single impedance. As such, the homogenized representation of Eq. 2 is crucial. However, its validity only holds in as much as the parallel assembly pattern size remains well below that of the wavelength. This pattern size can be defined as the characteristic length of the assembly. For instance, in the top view of such a meta-surface in Fig. 9, the characteristic length is L_c. For a meta-surface composed of 9 cells of 2cm by 2cm each, the characteristic size is 6cm, meaning that Eq. 2 holds for frequencies below ≈ 5.7kHz in air. More work is needed to check how much lower the frequency needs to be for the hypothesis to remain adequate.

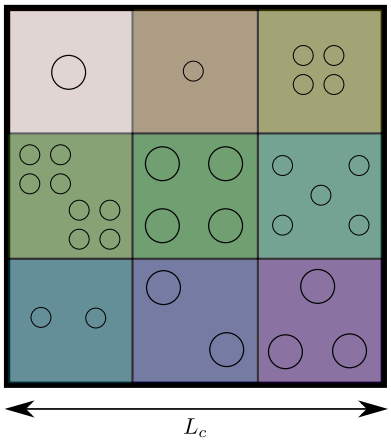

Figure 9: Top view of a meta-surface made of 9 different cells. L_c is the characteristic length of the meta-surface.

4. EXPERIMENTS ON A LINER META-SURFACE

We now leave the realm of numerical tests to try our hands on a real experiment. Using an earlier version of OPAL (using a 1D approximation from the *mamout* module instead of the *pyDG* module), a similar project was conducted in 2019 and is shown here as an example. The main goal was to reach a good absorption at 500Hz in ONERA's B2A aeroacoustic bench, while keeping the total sample thickness under 7cm. The chosen liner configuration is a meta-surface consisting of 3 different cells, each having 3 layers in a serial assembly (one SDOF and 2 LEONAR), see Fig. 10. The measured TLs are also given in Fig. 10, displaying a high absorption at low frequencies near 500Hz, and around 2kHz. Future prospects include a thorough experimental validation, now using the *pyDG* module for more accurate predictions of the TL.

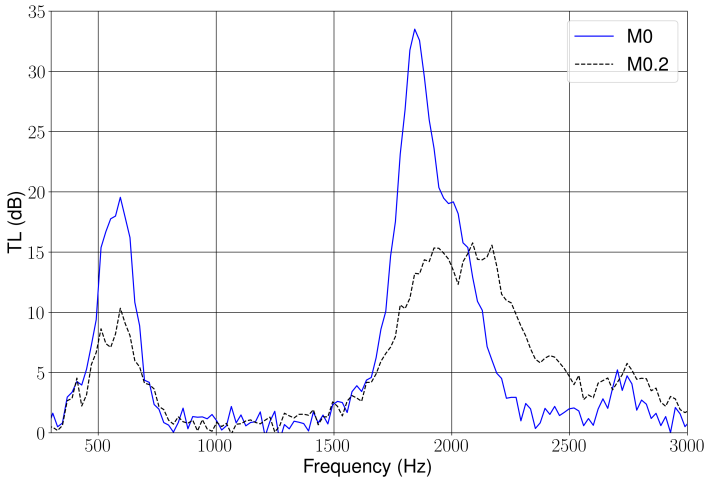

(a) Experimental TL obtained for an optimized meta-surface liner in the B2A aeroacoustic bench, at Mach 0 and Mach 0.2 (average).

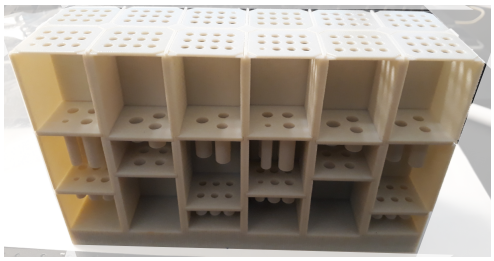

(b) 3D-printed sample.

Figure 10: Summary of the experiment. Transmission loss (left) and 3D printed sample (right).

5. DISCUSSION

The numerical case that was presented in Sec. 3 is a simplified version of what a real liner design project could be. In practice, multiple acoustic modes should be considered and the duct geometry would be more complex. Potentially, multiple impedance patches would be optimized simultaneously, with additional objectives (for instance, one could also try to minimize the waves reflected by the liner). All the elements to target these advanced problems are readily available in OPAL.

The purpose of the liner optimization procedure in Sec. 3 was not to declare a winner among all the combinations that were tested, as they all have their own merits. Depending on the environment (shear grazing flow, high SPL), the total available thickness and the target frequencies, liner candidates might perform better or worse than their counterparts. For instance, we have noticed that LEONAR materials showed a superior absorption at low frequencies when space constraints were tighter.

The current strategy allows the discrimination between all the potential candidates using fast and accurate evaluations of acoustic indicators obtained via 2D LEE calculations, only requiring a couple hours of sequential numerical work. This includes the generation of the snapshot-POD basis and the evaluation of the TL maps, which needs to be done only once for a given configuration (i.e., a given geometry and shear flow profile). The TL results displayed in Sec. 3 each take about 15min to be generated, using sequential optimization with pyMOO on a personal laptop.

6. CONCLUSIONS

An application of the OPAL software was presented, illustrating an acoustic liner design strategy. The main element of OPAL is the coupling between two modules. The first one, called *sandbox*, provides an acoustic liner library, extensible by the user to represent any liner made of acoustic unit elements that can be represented by a transfer matrix method. Then, the *pyDG* module allows 2D calculations of the LEE to solve for the acoustic field of a configuration, in the presence of a shear grazing flow. The library includes models from the literature to account for nonlinear effects caused by the presence of a flow and a high SPL. A numerical example was shown to mimic a liner design project in a small scale aeroacoustic bench, presenting the general strategy and the expected attenuation performed in the duct for three different meta-surface and multi-layer liners. First results of an experimental case were also presented, where the transmission loss was given for a complex meta-surface liner.

ACKNOWLEDGEMENTS

We gratefully acknowledge all the ONERA contributors involved in the DOCCLA project, framework of OPAL development.

REFERENCES

[1] Sjoerd W Rienstra. Fundamentals of duct acoustics. *Von Karman Institute Lecture Notes*, 2015.

[2] Pauli Virtanen and colleagues. SciPy 1.0: Fundamental Algorithms for Scientific Computing in Python. *Nature Methods*, 17:261–272, 2020.

[3] J. Blank and K. Deb. Pymoo: Multi-objective optimization in python. *IEEE Access*, 8:89497–89509, 2020.

[4] Jean Allard and Noureddine Atalla. *Propagation of Sound in Porous Media: Modelling Sound Absorbing Materials 2e*. John Wiley & Sons, New York, 2009.

[5] David Linton Johnson, Joel Koplik, and Roger Dashen. Theory of dynamic permeability and tortuosity in fluid-saturated porous media. *J. Fluid Mech.*, 176:379–402, 1987.

[6] Yvan Champoux and Jean-F Allard. Dynamic tortuosity and bulk modulus in air-saturated porous media. *J. Appl. Acoust.*, 70(4):1975–1979, 1991.

[7] Steven R Pride, Frank Dale Morgan, and Anthony F Gangi. Drag forces of porous-medium acoustics. *Phys. Rev. B*, 47(9):4964–4978, 1993.

[8] Denis Lafarge, Pavel Lemarinier, Jean F Allard, and Viggo Tarnow. Dynamic compressibility of air in porous structures at audible frequencies. *J. Acoust. Soc. Am.*, 102(4):1995–2006, 1997.

[9] Noureddine Atalla and Franck Sgard. Modeling of perforated plates and screens using rigid frame porous models. *Journal of sound and vibration*, 303(1-2):195–208, 2007.

[10] Frank Simon. Low frequency sound absorption of resonators with flexible tubes. In *Proceedings of Meetings on Acoustics ICA2013*, volume 19, page 030012. Acoustical Society of America, 2013.

[11] Frank Simon. Long elastic open neck acoustic resonator for low frequency absorption. *Journal of Sound and Vibration*, 421:1–16, 2018.

[12] Dengke Li, Daoqing Chang, and Bilong Liu. Enhancing the low frequency sound absorption of a perforated panel by parallel-arranged extended tubes. *Applied Acoustics*, 102:126–132, 2016.

[13] Thomas Henry Melling. The acoustic impendance of perforates at medium and high sound pressure levels. *J. Sound Vib.*, 29(1):1–65, 1973.

[14] AW Guess. Calculation of perforated plate liner parameters from specified acoustic resistance and reactance. *J. Sound Vib.*, 40(1):119–137, 1975.

[15] Muttalip Aşkın Temiz, Jonathan Tournadre, Ines Lopez Arteaga, and Avraham Hirschberg. Non-linear acoustic transfer impedance of micro-perforated plates with circular orifices. *Journal of Sound and Vibration*, 366:418–428, 2016.

[16] V Lafont, F Méry, R Roncen, F Simon, and E Piot. Liner impedance eduction under shear grazing flow at a high sound pressure level. *AIAA Journal*, 58(3):1107–1117, 2020.

[17] J. Primus, E. Piot, and F. Simon. An adjoint-based method for liner impedance eduction: Validation and numerical investigation. *J. Sound Vib.*, 332(1):58–75, January 2013.

[18] R Roncen, F Méry, E Piot, and F Simon. Statistical inference method for liner impedance eduction with a shear grazing flow. *AIAA Journal*, pages 1–11, 2018.

[19] Jan S Hesthaven and Tim Warburton. *Nodal discontinuous Galerkin methods: algorithms, analysis, and applications*. Springer Science & Business Media, 2007.

[20] Remi Roncen, Estelle Piot, Fabien Mery, Frank Simon, Michael G Jones, and Douglas M Nark. Influence of source propagation direction and shear flow profile in impedance eduction of acoustic liners. In *25th AIAA/CEAS Aeroacoustics Conference*, page 2469, 2019.

[21] René Pinnau. Model reduction via proper orthogonal decomposition. *Model Order Reduction: Theory, Research Aspects and Applications*, 13:95–109, 2008.

[22] Christophe Geuzaine and Jean-François Remacle. Gmsh: A 3-d finite element mesh generator with built-in pre-and post-processing facilities. *International journal for numerical methods in engineering*, 79(11):1309–1331, 2009.

[23] ME D'Elia, T Humbert, and Y Aurégan. Effect of flow on an array of helmholtz resonators: Is kevlar a "magic layer"? *The Journal of the Acoustical Society of America*, 148(6):3392–3396, 2020.